



FEM modeling and modal analysis of a cantilever beam

Master's Degree in Automotive Engineering

Loris Fonseca: s342696@studenti.polito.it

Nikoloz Kapanadze: s342649@studenti.polito.it

Maurizio Pio Vergara: s346643@studenti.polito.it

Renis Shtylla: s344685@studenti.polito.it

a.a 2024/2025

Contents

1	Introduction	3
2	Description of the system	3
3	Numerical FEM model of the cantilever beam	3
3.1	Evaluation of the stiffness and mass matrices	4
4	Mode shapes	6
5	Modal analysis	8
6	State space representation	10
7	Tuning of the parameters	12
7.1	Young's Modulus tuning	13
7.2	Damping Factor tuning	14
8	Conclusions	14

1 Introduction

Modal analysis is a fundamental technique used to study the dynamic behavior of structures and mechanical systems. It focuses on identifying the modal properties of a system, such as natural frequencies, mode shapes, and damping ratios. These properties are essential for understanding how a structure vibrates when subjected to dynamic forces. Through modal analysis it is possible to predict the system response to different excitation sources by identifying the resonance conditions that could lead to excessive vibrations. Therefore, the design can be optimized to enhance dynamic performance and minimize unwanted vibrations.

In this survey, a simple numerical model of a cantilever beam, obtained by means of a FEM approach, is studied through modal analysis, in order to evaluate the effect of the damping coefficient and the elastic modulus on its frequency response. The accuracy of the numerical results is then validated by comparing them with experimental data, in order to properly tune the model parameters and match the real ones.

2 Description of the system

The system to be modeled consists of an aluminum cantilever beam clamped on one side. The frequency response of the system is studied when an impulse force is applied on the beam itself. The properties of the beam are reported in Table 1.

l	280	mm	Length
w	30	mm	Width
t	3	mm	Thickness
ρ	2700	kg/m^3	Density
E	$70 \cdot 10^9$	N/m^2	Young modulus
ν	0.33	-	Poisson coefficient
Aluminum		Material	

Table 1: Cantilever beam properties

The following assumptions are made to simplify the model and the analysis:

- The material is homogeneous and isotropic
- The bending in the x axis and y axis are decoupled

Moreover, since this study requires only the evaluation of the vertical displacement and the rotation around the y -axis, the model can be studied by focusing on its 2D equivalent system. A representation of the beam model is depicted in Figure 1.

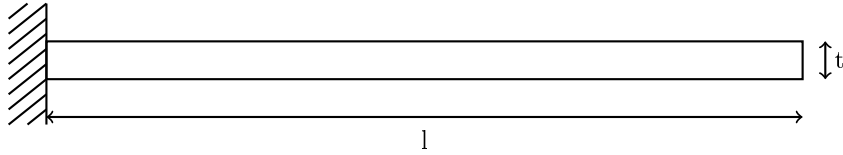


Figure 1: Cantilever beam 2D representation

3 Numerical FEM model of the cantilever beam

The first step of the analysis, in order to later find the mode shapes and the natural frequencies, is the creation of the numerical model of the cantilever beam. The model is discretized using the Finite Element Method (FEM) with 2D plate elements. Each element consists of two nodes, with each node having two degrees of freedom: displacement along the x -axis and rotation around the y -axis, as illustrated in Figure 2.

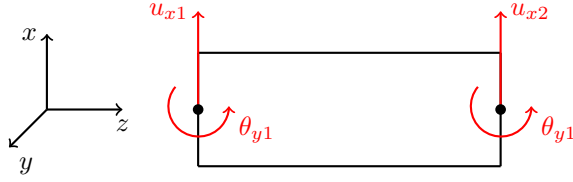


Figure 2: 2D element used to discretize the beam model

Therefore, the discretized cantilever beam can be analyzed by considering it as a system composed of N plate elements. In this survey, the cantilever beam is discretized using 28 elements, corresponding to 29 nodes. The resulting discretized model is depicted in Figure 3.

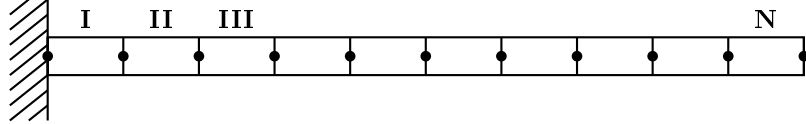


Figure 3: 2D discretized model of the cantilever beam

As a first approximation, the so obtained system can be represented as an assembly of massless springs and concentrated masses, located at the nodes of the model, as shown in Figure 4.

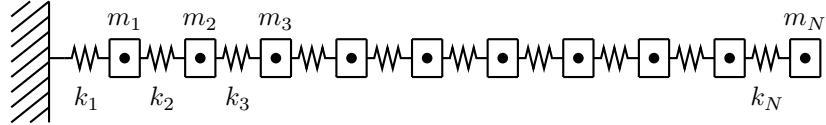


Figure 4: Cantilever beam mass-spring system

The dynamic behavior of the system is governed by the following equation:

$$[M]\{\ddot{q}\} + [C]\{\dot{q}\} + [K]\{q\} = \{F\} \quad (1)$$

Since the approximated system under study is assumed to be undamped and free from any external excitation, Equation 1 simplifies as follows:

$$[M]\{\ddot{q}\} + [K]\{q\} = \{F\} \rightarrow [M]\{\ddot{q}\} + [K]\{q\} = \{0\} \quad (2)$$

3.1 Evaluation of the stiffness and mass matrices

To obtain the mass and stiffness matrices of the beam, the first step to be performed is the calculation of the characteristic matrices for each plate element. These matrices describe the behavior of the individual element and depend on the material properties and geometry of the element. The stiffness and mass matrices of the single plate element are evaluated as follows:

$$K_i = \frac{E \cdot I_y}{l^3(1 + \phi_1)} \cdot \begin{bmatrix} 12 & 6l & -12 & 6l \\ 6l & (4 + \phi_1)l^2 & -6l & (2 - \phi_1)l^2 \\ -12 & -6l & 12 & -6l \\ 6l & (2 - \phi_1)l^2 & -6l & (4 + \phi_1)l^2 \end{bmatrix} \quad (3)$$

$$M_i = M_{i,1} + M_{i,2} \quad (4)$$

$$M_{i,1} = \frac{\rho \cdot A \cdot l}{420(1 + \phi_1)^2} \cdot \begin{bmatrix} m_1 & m_2 \cdot l & m_3 & -m_4 \cdot l \\ m_2 \cdot l & m_5 \cdot l^2 & m_4 \cdot l & -m_6 \cdot l^2 \\ m_3 & m_4 \cdot l & m_1 & -m_2 \cdot l \\ -m_4 \cdot l & -m_6 \cdot l^2 & -m_2 \cdot l & m_5 \cdot l^2 \end{bmatrix} \quad (5)$$

$$M_{i,2} = \frac{\rho \cdot I_y}{30l(1 + \phi_1)^2} \cdot \begin{bmatrix} m_7 & m_8 \cdot l & -m_7 & m_8 \cdot l \\ m_8 \cdot l & m_9 \cdot l^2 & -m_8 \cdot l & -m_{10} \cdot l^2 \\ -m_7 & -m_8 \cdot l & m_7 & -m_8 \cdot l \\ m_8 \cdot l & -m_{10} \cdot l^2 & -m_8 \cdot l & m_9 \cdot l^2 \end{bmatrix} \quad (6)$$

$$\begin{cases} \phi_1 = \frac{12EI_y\chi}{GAl^2} \\ m_1 = 156 + 294\phi_1 + 140\phi_1^2 \\ m_2 = 22 + 38.5\phi_1 + 17.5\phi_1^2 \\ m_3 = 54 + 126\phi_1 + 70\phi_1^2 \\ m_4 = 13 + 31.5\phi_1 + 17.5\phi_1^2 \\ m_5 = 4 + 7\phi_1 + 3.5\phi_1^2 \\ m_6 = 3 + 7\phi_1 + 3.5\phi_1^2 \\ m_7 = 36 \\ m_8 = 3 - 15\phi_1 \\ m_9 = 4 + 5\phi_1 + 10\phi_1^2 \\ m_{10} = 1 + 5\phi_1 - 5\phi_1^2 \end{cases} \quad (7)$$

Once the local matrices are computed, they are combined to form the global stiffness and mass matrices of the entire beam. This assembly process is based on the common nodes and degrees of freedom shared between the elements. By aligning the local DOFs with their corresponding global DOFs and summing the contributions from each element at the shared nodes, the complete mass and stiffness matrices for the entire beam are constructed, as represented in Figure 5. This process ensures that the interactions and constraints at the shared nodes are accurately represented in the overall structural model. Since this study involves 29 nodes, each with 2 degrees of freedom, the stiffness and mass matrices are both 58x58 square matrices.

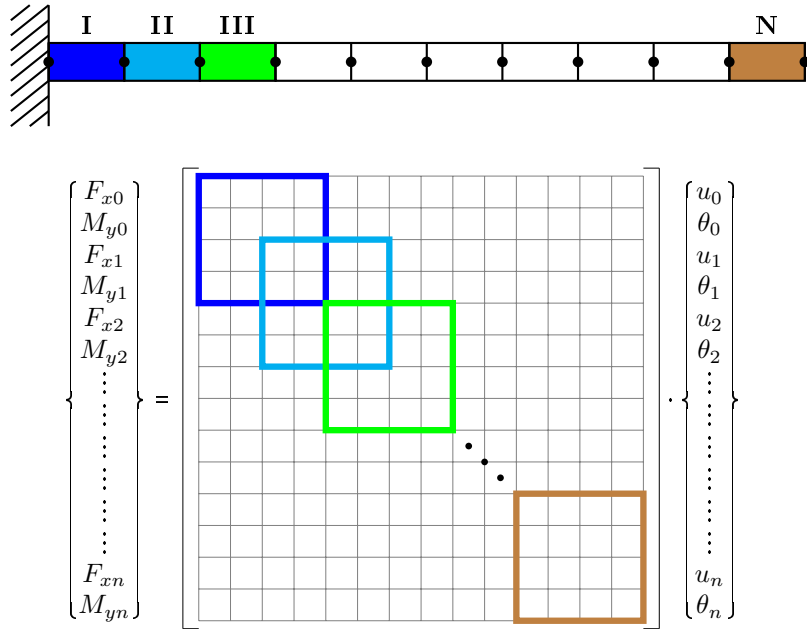


Figure 5: Global stiffness matrix evaluation

A further simplification can be applied to the system: since the left end of the beam is fully clamped, the displacement and rotation at node 0 are null. Therefore, the order of stiffness and mass matrices can be reduced by removing the rows and columns associated with the degrees of freedom at node 0 (u_0 and θ_0). This reduction decreases the overall degrees of freedom of the system, thereby simplifying it, as illustrated in Figure 6.

$$\begin{bmatrix} F_{x0} \\ M_{y0} \\ F_{x1} \\ M_{y1} \\ F_{x2} \\ M_{y2} \\ \vdots \\ F_{xn} \\ M_{yn} \end{bmatrix} = \begin{bmatrix} & & & & & & & \\ & \text{blue box} & & & & & & \\ & & \text{cyan box} & & & & & \\ & & & \text{green box} & & & & \\ & & & & \ddots & & & \\ & & & & & \ddots & & \\ & & & & & & \text{orange box} & \\ & & & & & & & \end{bmatrix} \cdot \begin{bmatrix} u_0 \\ \theta_0 \\ u_1 \\ \theta_1 \\ u_2 \\ \theta_2 \\ \vdots \\ u_n \\ \theta_n \end{bmatrix}$$

Figure 6: Global stiffness matrix simplification

Consequently, the system order in the analyzed case is reduced from 58 to 56. It is also important to note that, since the experimental data are obtained using an accelerometer mounted directly on the beam, its mass must be accounted for when evaluating the mass matrix. Specifically, the accelerometer is mounted at node 11, and its mass is incorporated into the matrix coefficient corresponding to its degree of freedom, namely entry (21,21) of the mass matrix.

4 Mode shapes

Once the mass and stiffness matrices of the entire beam are evaluated, Equation 2 can be solved, finding the mode shapes and the natural frequencies of the studied system. Mode shapes represent the characteristic deformation patterns of the beam when it vibrates. Each mode shape corresponds to a specific natural frequency, and it illustrates how the different nodes along the beam move relative to each other. Correspondingly, natural frequencies are the specific frequencies at which the different mode shapes of the system tends to oscillate when an external excitation is applied to the system itself.

In the context of the Frequency Response Function (FRF), which describes how the output of a system responds to an input across different frequencies, peaks are observed at the system's resonance frequencies. These peaks indicate that the system exhibits maximum amplitude at its natural frequencies due to resonance, where the input frequency matches the system's natural oscillatory behavior. A qualitative representation of a FRF is depicted in Figure 7, where the natural frequencies of the system are visible in correspondence of the function's peaks.

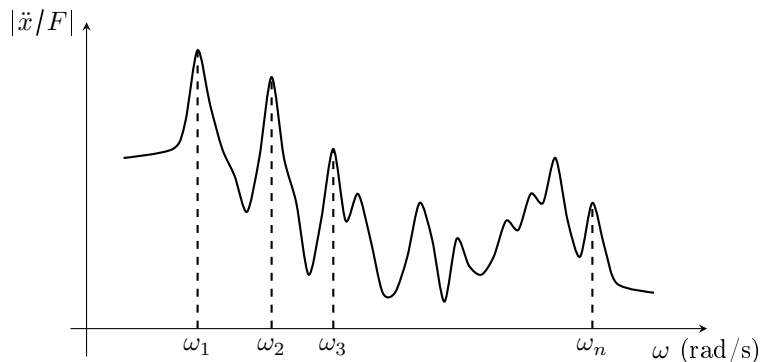


Figure 7: Qualitative representation of a Frequency Response Function

The analytical solution of the system's equation, along with its first and second derivatives, is presented in Equation 8.

$$\begin{cases} \{q(t)\} = \{q_0\} e^{i\omega t} \\ \{\dot{q}(t)\} = \{q_0\} i\omega e^{i\omega t} \\ \{\ddot{q}(t)\} = -\{q_0\} \omega^2 e^{i\omega t} \end{cases} \quad (8)$$

By substituting the analytical solution into system dynamic equation, the following relation is obtained:

$$\begin{aligned} -[M]\{q_0\}\omega^2 e^{i\omega t} + [K]\{q_0\}e^{i\omega t} &= \{0\} \rightarrow -[M]\{q_0\}\omega^2 e^{i\omega t} + [K]\{q_0\}e^{i\omega t} = \{0\} \\ \rightarrow -[M]\{q_0\}\omega^2 + [K]\{q_0\} &= \{0\} \rightarrow (-[M]\omega^2 + [K])\{q_0\} = \{0\} \end{aligned}$$

The evaluated equation is characterized by two solutions, listed as follows:

$$\begin{aligned} \{q_0\} &= \{0\} \\ -[M]\omega^2 + [K] &= \{0\} \end{aligned}$$

The first solution is called trivial solution, since it does not provide any information about the system's response. On the other hand, the second solution can be solved in order to determine the dynamic behavior of the analyzed system.

$$\begin{aligned} -[M]\omega^2 + [K] &= \{0\} \rightarrow [M]^{-1}(-[M]\omega^2 + [K]) = \{0\} \rightarrow [M]^{-1}[K] - \omega^2[I] = \{0\} \\ \rightarrow \det([M]^{-1}[K] - \omega^2[I]) &= 0 \end{aligned} \quad (9)$$

Solving Equation 9 is equivalent to solving the eigenproblem, which involves determining the eigenvalues and eigenvectors of the matrix $[M]^{-1}[K]$. In the case of the system under analysis, the eigenvalues correspond to the squares of the system's natural frequencies, while the eigenvectors represent the initial conditions for displacement along the x -axis and rotation about the y -axis at the respective natural frequencies, i.e. the mode shapes of the system.

For the analyzed system, a clamped cantilever beam subjected to an impulse force, the first three and the last resonance frequency are the following:

$$\omega_1 = 186 \text{ rad/s}, \quad \omega_2 = 996 \text{ rad/s}, \quad \omega_3 = 2895 \text{ rad/s}, \quad \omega_n = 2.08 \cdot 10^6 \text{ rad/s}$$

Instead, the representation of the eigenvectors is shown in Figure 8, 9 and 10. These pictures illustrate the first, second and third mode shapes of the system, corresponding to the deformed shape of the beam when oscillating at its first, second and third resonance frequency, respectively.

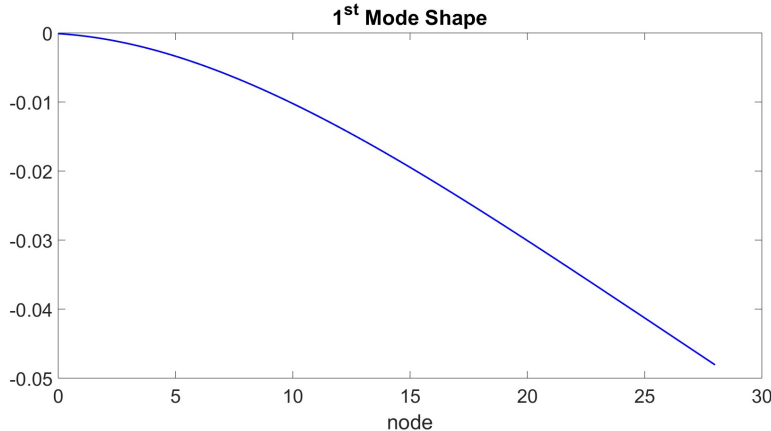


Figure 8: First mode shape of the cantilever beam

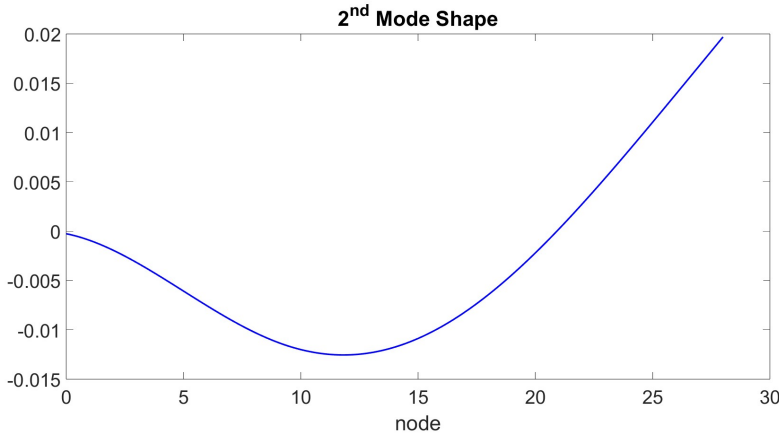


Figure 9: Second mode shape of the cantilever beam

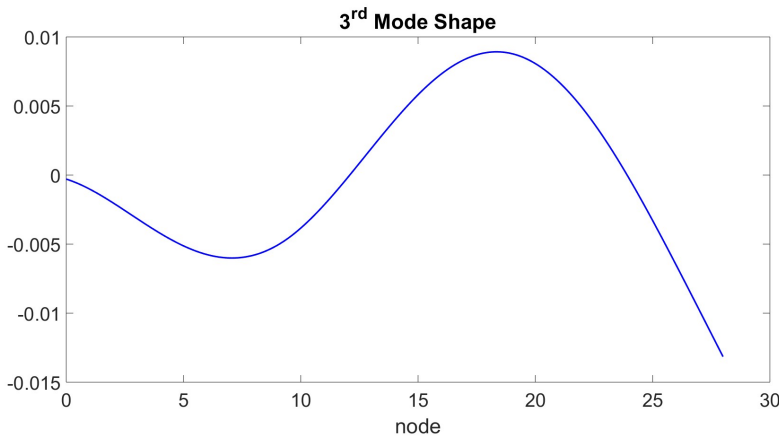


Figure 10: Third mode shape of the cantilever beam

It can be noticed that the first mode involves a smooth, large deflection near the free end, while higher modes exhibit increasingly complex oscillatory patterns. These shapes are characteristic of a cantilever beam and depend on beam's material properties, geometry, and boundary conditions.

5 Modal analysis

In the previous sections, the analysis focused on a system composed only of masses and stiffnesses. However, the real system exhibits also damping, which must be taken into account when studying the dynamic response of the system. Unlike mass and stiffness, the damping values are unknown and cannot be directly calculated. Instead, they must be determined by comparing the theoretical results with experimental data. This process requires tuning the damping matrix element by element and iteratively match the outcomes with experimental results, adjusting its values to minimize the discrepancy between the theoretical and experimental data.

Given the large dimension of the system, the size of the damping matrix is huge, making direct tuning in the physical coordinates very time-consuming. To overcome this problem, modal analysis is exploited to simplify the system. This analysis involves a modal transformation which translates the system into its modal coordinates. This transformation allows to decouple the degrees of freedom, resulting in independent modal components.

Therefore, the matrices become diagonal, in the case of mass and stiffness matrices, or nearly diagonal, in the case of damping matrix. This diagonalization drastically reduces the complexity of the problem, as each mode can be analyzed independently. Consequently, tuning the damping parameters in modal space becomes much more effective, as it eliminates the need to consider cross-coupling terms between modes.

By treating the degrees of freedom as decoupled, instead of analyzing the beam as a whole, the system is transformed into an equivalent model where the degrees of freedom of each element are studied independently. As a result, the cantilever beam can be expressed as an equivalent system

comprising a series of individual mass-spring systems, with each of them representing a discrete segment of the beam.

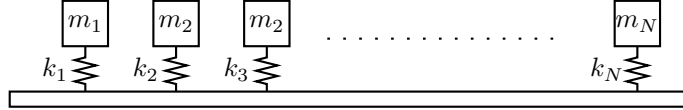


Figure 11: Equivalent decoupled mass-spring system of the cantilever beam

The modal transformation used for translating the system from physical coordinates to modal coordinates is the following:

$$\begin{cases} q = \phi \cdot \xi \\ \dot{q} = \phi \cdot \dot{\xi} \\ \ddot{q} = \phi \cdot \ddot{\xi} \end{cases} \quad (10)$$

It should be noted that, although with modal analysis the system is considered to be damped, since the damping values are small, the vector ϕ still represents the eigenvectors of the undamped system, evaluated in Section 4. By applying the modal transformation to Equation 1, which is expressed in physical coordinates, the equation of the system in modal coordinates is obtained:

$$[M]\phi\{\ddot{\xi}\} + [C]\phi\{\dot{\xi}\} + [K]\phi\{\xi\} = \{F\} \quad (11)$$

In order to obtain diagonal matrices, the orthogonality property of mass and stiffness matrices can be exploited. This property stands as follows:

$$\begin{cases} \phi^T [M] \phi = 0 & \text{if } i \neq j \\ \phi^T [K] \phi = 0 \end{cases}$$

Therefore, by multiplying both sides of Equation 11 by ϕ^T , the following equation is obtained:

$$\begin{aligned} \phi^T [M]\phi\{\ddot{\xi}\} + \phi^T [C]\phi\{\dot{\xi}\} + \phi^T [K]\phi\{\xi\} &= \phi^T \{F\} \\ \rightarrow [M]_{modal}\{\ddot{\xi}\} + [C]_{modal}\{\dot{\xi}\} + [K]_{modal}\{\xi\} &= \phi^T \{F\} \end{aligned} \quad (12)$$

where:

$$[M]_{modal} = \begin{bmatrix} m_{1,modal} & 0 & \cdots & 0 \\ 0 & m_{2,modal} & \cdots & 0 \\ \vdots & \vdots & \ddots & 0 \\ 0 & 0 & 0 & m_{n,modal} \end{bmatrix}$$

$$[K]_{modal} = \begin{bmatrix} k_{1,modal} & 0 & \cdots & 0 \\ 0 & k_{2,modal} & \cdots & 0 \\ \vdots & \vdots & \ddots & 0 \\ 0 & 0 & 0 & k_{n,modal} \end{bmatrix}$$

Mathematically, $[C]_{modal}$ is not diagonal. However, as previously mentioned, since the damping values are small, the off-diagonal terms can be considered negligible. Therefore, for the purposes of this study, the damping modal matrix is also assumed to be diagonal.

$$[C]_{modal} = \begin{bmatrix} c_{1,modal} & 0 & \cdots & 0 \\ 0 & c_{2,modal} & \cdots & 0 \\ \vdots & \vdots & \ddots & 0 \\ 0 & 0 & 0 & c_{n,modal} \end{bmatrix}$$

The damping terms on the diagonal can be expressed as follows:

$$c_{i,modal} = \zeta_{i,modal} \cdot c_{cr,i} \quad (13)$$

where $\zeta_{i,modal}$ is the damping factor, and $c_{cr,i}$ is the critical damping corresponding to the relative mode shapes, evaluated as:

$$c_{cr,i} = 2\sqrt{k_{i,modal} \cdot m_{i,modal}} \quad (14)$$

In this study, since the material is considered to be homogeneous and isotropic, the damping ratio is assumed to be the same for each mode of vibration. Therefore, the damping modal matrix can be expressed as:

$$[C]_{modal} = 2 \cdot \zeta \begin{bmatrix} \sqrt{k_{1,modal} \cdot m_{1,modal}} & 0 & \cdots & 0 \\ 0 & \sqrt{k_{2,modal} \cdot m_{2,modal}} & \cdots & 0 \\ \vdots & \vdots & \ddots & 0 \\ 0 & 0 & 0 & \sqrt{k_{n,modal} \cdot m_{n,modal}} \end{bmatrix}$$

The only unknown variable is ζ , which is the parameter to be tuned in order to achieve the matching between the theoretical results and the experimental data.

After obtaining the modal damping matrix, to evaluate the equivalent damping matrix of the real system in physical coordinates, the inverse modal transformation has to be applied:

$$\begin{aligned} [C]_{modal} &= [\phi]^T [C] [\phi] \rightarrow [C]_{modal} \cdot [\phi]^{-1} = [\phi]^T [C] [\phi] \cdot [\phi]^{-1} = [\phi]^T [C] [\phi] \cancel{[\phi]^{-1}} \\ &\rightarrow [C]_{modal} [\phi]^{-1} = [\phi]^T [C] \rightarrow ([\phi]^T)^{-1} [C]_{modal} [\phi]^{-1} = ([\phi]^T)^{-1} [\phi]^T [C] = \cancel{([\phi]^T)^{-1}} [\phi]^T [C] \\ &\rightarrow [C] = ([\phi]^T)^{-1} [C]_{modal} [\phi]^{-1} \end{aligned} \quad (15)$$

6 State space representation

Once the matrices of mass, stiffness and damping are computed by exploiting the simplification provided by the modal transformation, the system can be expressed in terms of state space representation. This representation provides a convenient way to analyze the dynamic behavior of the beam in terms of its internal state variables. In the state space framework, a system is described by a set of first-order differential equations. The state variables form a vector, and the system's evolution over time is governed by a matrix equation. This representation is typically expressed in two key equations: the State Equation and the Output Equation, reported in Equation 16.

$$\begin{cases} \dot{x}(t) = Ax(t) + Bu(t) \\ y(t) = Cx(t) + Du(t) \end{cases} \quad (16)$$

where:

- $x(t)$ is the state vector, representing the system's internal state at time t
- A is the state matrix, defining the relationships among the states
- $u(t)$ is the input vector, representing external influences on the system
- B is the input matrix, mapping inputs to state changes
- $y(t)$ is the output vector, representing the system's measurable outputs
- C is the output matrix, linking states to outputs
- D is the feedthrough matrix, describing direct input-to-output effects

Since the studied system is a second order system, the state vector is characterized by two states:

$$x = \begin{pmatrix} x_1 \\ x_2 \end{pmatrix} = \begin{pmatrix} \{q\} \\ \{\dot{q}\} \end{pmatrix} = \begin{pmatrix} \left\{ \begin{array}{c} u_1 \\ \theta_1 \\ \vdots \\ u_n \\ \theta_n \\ \dot{u}_1 \\ \dot{\theta}_1 \\ \vdots \\ \dot{u}_n \\ \dot{\theta}_n \end{array} \right\} \end{pmatrix} \quad (17)$$

Therefore, by exploiting Equation 1, the derivative of the state vector can be expressed as follows:

$$\dot{x} = \begin{pmatrix} \dot{x}_1 \\ \dot{x}_2 \end{pmatrix} = \begin{pmatrix} \{\dot{q}\} \\ \{\ddot{q}\} \end{pmatrix} = \begin{pmatrix} x_1 \\ -[M]^{-1}[K]x_1 - [M]^{-1}[C]x_2 + [M]^{-1}\{F\} \end{pmatrix} \quad (18)$$

Once the state variables are expressed, the matrices A and B can be computed. In particular:

$$A = \begin{bmatrix} 0 & I \\ -M^{-1}K & -M^{-1}C \end{bmatrix} \quad (19)$$

$$B = \begin{bmatrix} 0 \\ M^{-1} \end{bmatrix}$$

where I is the identity matrix.

Thus, the state equation describing the cantilever beam dynamic has this form:

$$\begin{pmatrix} \{\dot{q}\} \\ \{\ddot{q}\} \end{pmatrix} = \begin{bmatrix} 0 & I \\ -M^{-1}K & -M^{-1}C \end{bmatrix} \begin{pmatrix} \{q\} \\ \{\dot{q}\} \end{pmatrix} + \begin{bmatrix} 0 \\ M^{-1} \end{bmatrix} \{F\} \quad (20)$$

To establish a correspondence between the analytical values and the experimental data, and ensure an accurate comparison, the matrices characterizing the output equation must be constructed according to the experimental procedure used to collect the data. Specifically, C and D correspond to the rows of A and B relative to the x -axis acceleration of the node where the accelerometer is mounted during the experimental test. This means that y is simply equal to \ddot{u}_{acc} .

Once the state-space matrices are determined, the Frequency Response Function (FRF) of the system can be plotted using the Bode diagram, as shown in Figure 12.

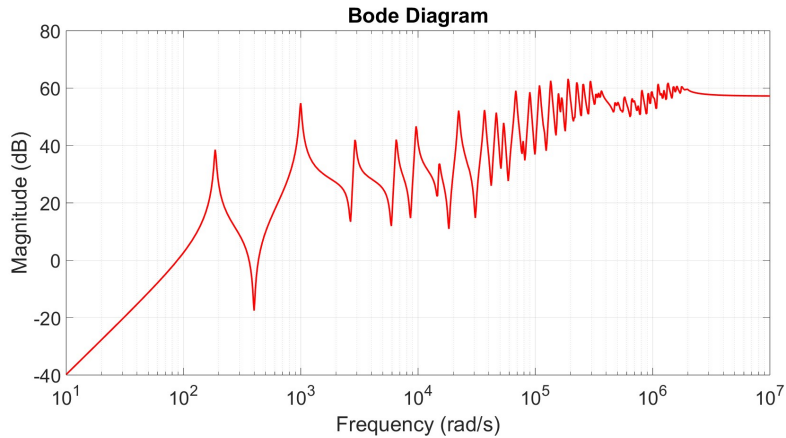


Figure 12: Analytical FRF of the cantilever beam

It should be noted that the resulting function exhibits a series of peaks, each of them corresponding to the resonance frequency specific of a particular mode shape. Therefore, the accuracy of the Frequency Response Function and the effectiveness of the modal analysis can be easily evaluated by comparing the resonance frequencies identified from the FRF graph with those derived from the mode shape analysis. These two sets of resonance frequencies should match. In Figure 13, the first three and the last resonance frequencies, graphically determined, are reported. The obtained values correspond to those presented in Section 4, calculated by solving the eigenproblem. The consistency between these values confirms the validity of the FRF and ensures that the system's dynamic behavior is accurately captured.

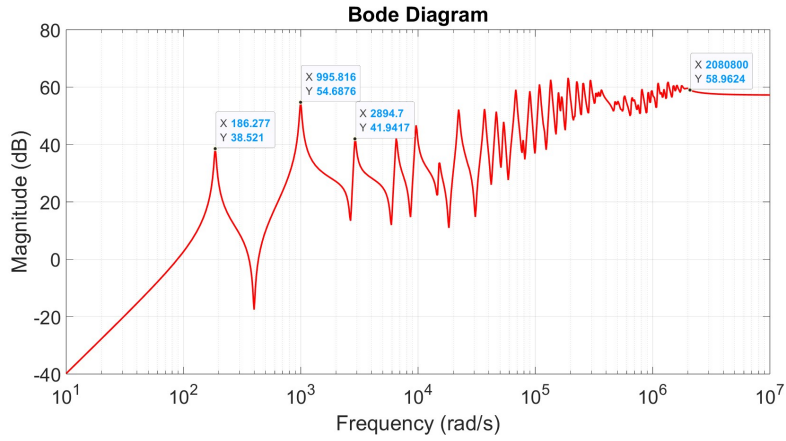


Figure 13: Graphically determined resonance frequency values from the FRF

7 Tuning of the parameters

The final step in this analysis is tuning the system parameters in order to match the experimental data with the analytical result. In particular, two types of discrepancies are observed between the experimental and analytical charts: (i) the resonance frequencies, i.e. the frequency values at which dynamic response is characterized by a peak, and (ii) the magnitude of the peak values in correspondence of the resonance frequencies.

As shown in Figure 14, experimental data acquisition is limited to frequencies up to 400 Hz, as the dynamic response of the analyzed mechanical system beyond this range is not significant. Therefore, the previously obtained Frequency Response Function is constrained to this range and translated into a Hertz scale, as illustrated in Figure 15. As a consequence, parameter identification is confined to the first two mode shapes of the system.

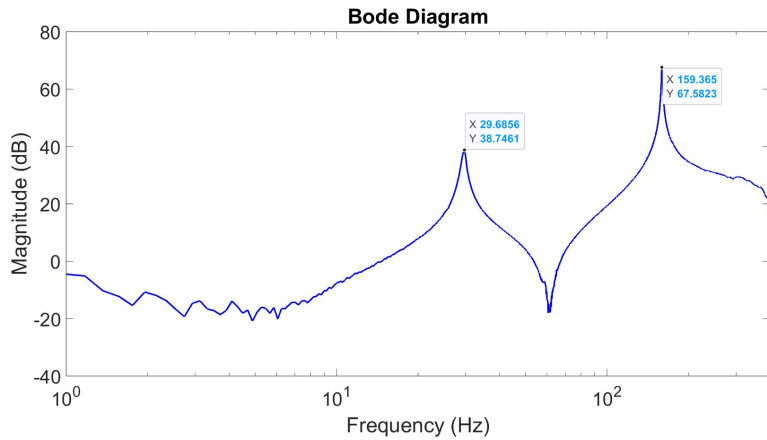


Figure 14: Experimental FRF of the cantilever beam

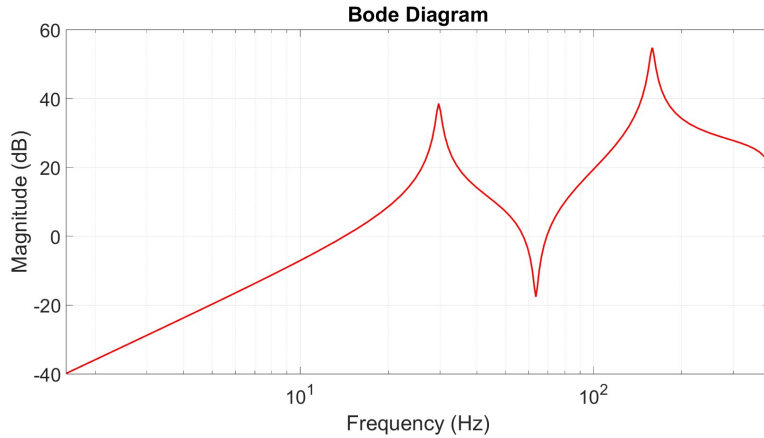


Figure 15: FRF of the system, constrained to a frequency range of up to 400 Hz

The comparison between the analytically evaluated FRF and the experimental FRF is shown in Figure 16.

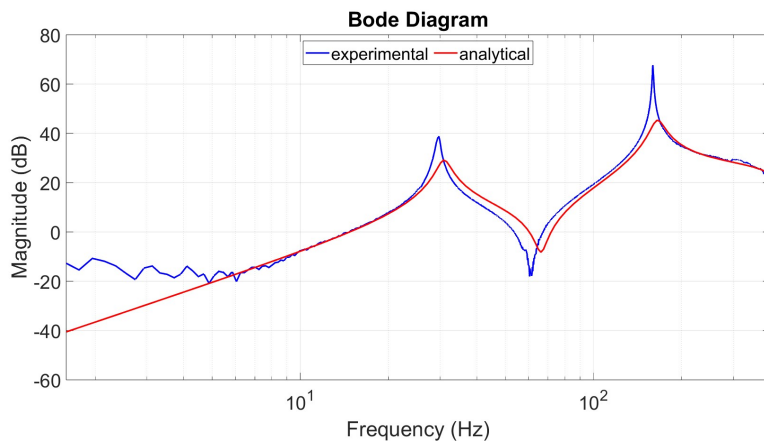


Figure 16: Comparison between analytical and experimental FRF

7.1 Young's Modulus tuning

The resonance frequency is proportionally related to the ratio between stiffness and mass. Therefore, frequency discrepancy can be tuned by modifying this ratio. Since the mass value is measured and known, the only source of uncertainty is the stiffness value, which instead is not precisely measured. As a result, the resonance frequencies of the analytical chart are adjusted to match those of the experimental chart by modifying the stiffness values, which are directly related to the Young Modulus, as expressed by Equation 3. Following this procedure, the resulting Young's Modulus is determined to be:

$$E = 64.5 \cdot 10^9 N/m^2$$

The chart obtained after tuning the Young's Modulus is depicted in Figure 17, illustrating the alignment between the peaks of the experimental and analytical charts.

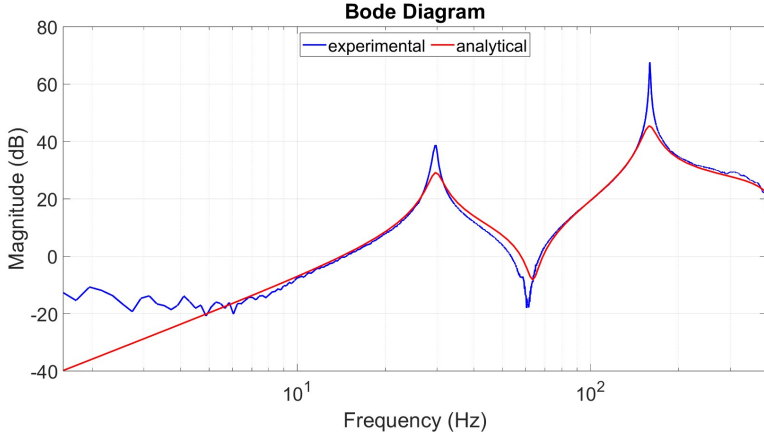


Figure 17: FRF comparison after Young’s Modulus tuning

7.2 Damping Factor tuning

The second parameter to be tuned to obtain a correspondence between the experimental and the analytical results is the damping factor ζ . By applying a trial-and-error procedure, it is found that the value of the damping factor minimizing the error between the experimental and analytical charts is the following:

$$\zeta = 0.017$$

The final result is shown in Figure 18.

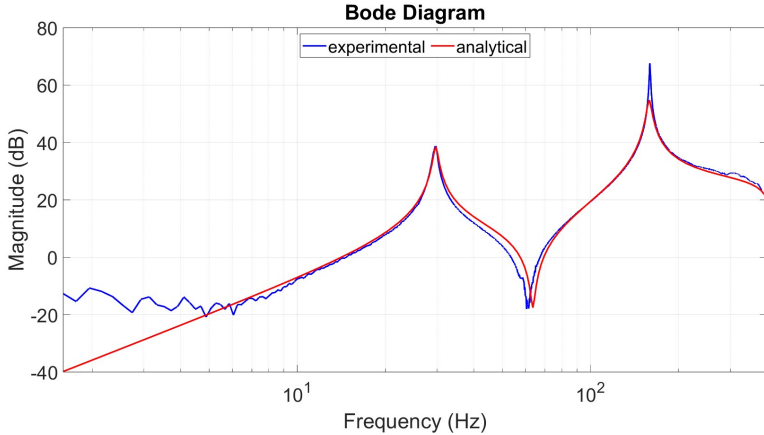


Figure 18: FRF comparison after damping factor tuning

It should be noted that the tuning of the Young’s Modulus and the damping factor is primarily focused on achieving a match at the first resonance frequency, as it represents the most significant dynamic behavior of the system. This resonance dominates the system’s response, making it the critical focus for calibration. Indeed, as shown in the chart in Figure 18, the experimental and analytical curves overlap almost perfectly at the first resonance frequency. However, a slight discrepancy remains at the second resonance frequency, where the two curves are not entirely aligned.

8 Conclusions

The modal analysis and parameter tuning of the cantilever beam conducted in this study provided valuable insights into the dynamic behavior of the system. A numerical model was successfully developed using the Finite Element Method (FEM) to evaluate the stiffness and mass matrices, natural frequencies, and mode shapes. Experimental data were employed to fine-tune the model’s parameters by exploiting modal analysis, ensuring that the theoretical results closely matched the real-world observations.

The study demonstrates the robustness of FEM in dynamic analysis and underscores the importance of experimental validation in achieving accurate system modeling.